

SOLIDIFICATION OF BOF SLAGS MODIFIED BY PYROMETALURGY AND SUBMITTED AT DIFFERENT COOLING RATES

Antonio Malynowskyj¹
Marcelo Breda Mourão¹
João Batista Ferreira Neto^{2,3}
Fabiano Ferreira Chotoli^{2,3}

Abstract

In a scenario of blast furnace slag shortage, the use of BOF slag (Blast Oxygen Furnace) as a partial substitute in cement production is a low cost alternative. In this paper, BOF (Blast Oxygen Furnace) slag samples were melted in an experimental electric arc furnace (EAF), with different modifiers materials (Al top dross reject, slag from FeSi iron alloy production, et al.) with different rates of additions, subject to differentiated cooling in specifically designed experimental apparatus. The objective was to search the formation of different phases formed during a process of BOF slag modification, for different materials additions containing Al_2O_3 and SiO_2 and subjected to different cooling conditions. Modified slags, with basicity (CaO/SiO_2) below 1.1 and Al_2O_3 contents less than 5%, subjected to cooling rates up to $21^\circ C/s$, favor the formation of crystalline phases; no amorphous phases were detected in this trial. Modified slag tests with basicity below 1.2 and Al_2O_3 content between 10.0% and 12.5% favor both the formation of crystalline (majority) and amorphous phases (between 25% and 30%). The influence of the cooling rate up to $21^\circ C/s$ on amorphous phase formation in this trial was not conclusive.

Keywords: BOF slag; Slag cooling; Microstructure; Thermodynamic simulation.

SOLIDIFICAÇÃO DE ESCÓRIAS BOF MODIFICADAS POR PIROMETALURGIA E SUBMETIDAS A DIFERENTES TAXAS DE RESFRIAMENTO

Resumo

Em um cenário de escassez de escória de alto forno, o uso de escória BOF (Blast Oxygen Furnace) como substituto parcial na produção de cimento, é uma alternativa de baixo custo. Neste trabalho, foram fundidas amostras de escórias BOF em forno elétrico a arco (FEA) experimental, com diferentes materiais modificadores (borra de Al, escória de fabricação de Fe-Si, entre outros), e submetidos a resfriamento diferenciado, em aparatos experimentais especificamente projetados. O objetivo foi pesquisar a formação das fases formadas durante um processo de modificação de escórias BOF, por adições de diferentes materiais contendo Al_2O_3 e SiO_2 e submetidos a diferentes taxas de resfriamento. Escórias modificadas, com basicidade (CaO/SiO_2) abaixo de 1,1 e teores de Al_2O_3 inferior a 5%, submetidas a taxas de resfriamento de até $21^\circ C/s$, favorecem a formação de fases cristalinas; não foram detectadas fases amorfas neste grupo de ensaio. Ensaios de escórias modificadas com basicidade abaixo de 1,2 e teores de Al_2O_3 entre 10,0%, e 12,5%, favorecem a formação tanto de fases cristalinas (majoritária) quanto de fase amorfa (entre 25% e 31%). A influência da taxa de resfriamento de até $21^\circ C/s$ na formação de fase amorfa, neste grupo de ensaios não foi conclusiva.

Palavras-chave: Escória BOF; Resfriamento escória; Microestrutura; Simulação termodinâmica.

¹Departamento de Engenharia Metalúrgica e de Materiais, Escola Politécnica, Universidade de São Paulo – USP, São Paulo, SP, Brasil.
E-mail: antoniomaly15@gmail.com

²Laboratório de Processos Metalúrgicos – LPM, Instituto de Pesquisas Tecnológicas – IPT, São Paulo, SP, Brasil.

³Laboratório de Materiais de Construção Civil – LMCC, Instituto de Pesquisas Tecnológicas – IPT, São Paulo, SP, Brasil.



I INTRODUCTION

Slag from the BOF process usually accounts for between 9 and 15% of liquid steel production, and is an important component in the primary refinery stage of a steelworks. However, in the current state-of-the-art, the vast majority are discarded, although there is a large literature on the subject of their reuse, a robust and consistent solution is not yet agreed [1-5]. The use of industrial waste as a raw material for the manufacture of cement has stood out in the cement industry, which research viable alternatives and the slag BOF process is one of the most investigated. Blast furnace slag is the most used in cement production, due to the favorable proximity of its chemical composition to that of Portland cement, besides having satisfactory hydraulic reactivity. In Brazil, steel production is stagnant, but civil construction, a major consumer of cement, is being demanded, so that the substitution of blast furnace slag for BOF slag would be a low cost strategic response.

The BOF slags, although they present chemical components common to Portland cement have serious restrictions regarding their use in the construction industry due to the expansion caused by the oxidation of Iron (Fe^0 and Fe^{+2}) and CaO-free and MgO-free expansion effect after hydration [6]. In the HBM process described by Yao-Hung Tseng et al., oxygen and SiO_2 are injected into the liquid slag in order to reduce basicity and inhibit the formation of CaO-free and MgO-free, enabling this material for many applications [7].

The BOF slag is of a basic and oxidizing nature, and for the Brazilian current steel mills conditions, it has in its chemical composition: CaO 35-40%, SiO_2 10-15%, MgO 9-15%, P_2O_5 1-2% and total iron (in the form of Fe^{+2} , Fe^{+3} and Fe^0) of the order of 19 to 25%. Certain crystallographic phases may favor the cementitious properties of BOF slags like Belite ($2\text{CaO}\cdot\text{SiO}_2$) and Alite ($3\text{CaO}\cdot\text{SiO}_2$). Another factor is the influence of the different cooling rates of the liquid slag, i.e., BOF slags that are air-cooled, are generally inert due to the crystallization of their oxides. Blast furnace slag has significant cementitious properties, because when submitted to granulation by high cooling rates, besides the high proportion of amorphous phase, they it contains Alite and Belite.

The mineral composition of the BOF slag could contain an amorphous and a crystalline part [8]. The crystalline part of the slag may contain solutions and solid precipitates. The main solutions found are Olivine solution, as Monticellite (CaMgSiO_4), Forsterite (Mg_2SiO_4), Faialite (Fe_2SiO_4), Tefroite (Mn_2SiO_4), Kirschsteinite (CaFeSiO_4) and Larnite (Ca_2SiO_4); Melilite solution, as Gehlenite ($\text{Ca}_2\text{Al}_2\text{SiO}_7$), and Akermanite ($\text{Ca}_2\text{MgSi}_2\text{O}_8$); Solid Monoxide Solution, also known as RO Phase, as Wüstite (Fe_xO), Lime (CaO) and Periclase (MgO).

The major pure solid precipitates that can be observed within a BOF slag are: Merwinite ($\text{Ca}_3\text{MgSi}_2\text{O}_8$), Belite (2CaO .

SiO_2) Alite ($3\text{CaO}\cdot\text{SiO}_2$) CaO-free, MgO-free, Brownmillerite ($\text{Ca}_2(\text{Al}, \text{Fe}^{+3})_2\text{O}_5$) and Srebrodolskite ($\text{Ca}_2\text{Fe}^{+3}_2\text{O}_5$).

2 MATERIALS AND METHODS

2.1 Design of Experiments

The strategies used in the design of experiments for slag modification were as follows: avoid CaO-free and MgO-free formation; reduce basicity, aiming to replicate blast furnace slag by adjusting the SiO_2 content; adjust the Al_2O_3 content of the slag, targeting blast furnace slag level.

The starting point for dimensioning the experiments were the ternary/ quaternary diagrams of the CaO-SiO₂-MgO system [2], taking into account contents of 0%, 5% and 10% of Al_2O_3 . With these parameters, the CaO-free and MgO-free fields disappear with the increase of Al_2O_3 . In ternary diagrams for 15%, 20%, 30% and 35% Al_2O_3 this trend continues. Another observation is that above 10% of Al_2O_3 , Monticellite is no longer the most stable phase, turning into Spinel, this phase being the predominant, from Al_2O_3 contents above 30% in the CaO-SiO₂-MgO system.

Thus, it was possible to predict trends for mineralogical phases that would be present in the modified slag, as shown in Table I. In this way, the criteria that met the premises mentioned in this topic were established in the design of experiments: basicity lower than 1.1 and MgO content less than 10% and increase in Al_2O_3 content.

A total of fifteen modification tests were carried out in BOF slags, and these were divided into two groups: Crystalline trials (12 heats), which aimed to reduce the initial basicity slag to lower values than 1.1. Second group called Amorphous trials (3 heats), which had as objective to increase the content of Al_2O_3 above 10% maintaining also in this case, the reduction of basicity to values below 1.1.

2.2 Slag Modification Pyrometallurgy

A batch of 5t of solid BOF slag and granulometry between 10 and 30mm, was obtained from COSIPA steel mill, located in São Paulo, Brazil. This material was re-melted in an experimental EAF with 300kg nominal capacity, using

Table I. CaO-SiO₂-MgO system, with 0%, 5% and 10% Al_2O_3 , basicity < 1.0 and MgO < 10%

Ternary System	Possible Mineralogical Phases
CaO-SiO ₂ -MgO System, for 0% Al_2O_3	Wollastonite, Akermanite
CaO-SiO ₂ -MgO system, to 5% Al_2O_3	Belite, Rankinite, Melilite, Pseudowollastonite, Monticellite, Merwinite
CaO-SiO ₂ -MgO system, for 10% Al_2O_3	Belite, Rankinite, Melilite, Pseudowollastonite

refractories based on MgO-C (17% C), quite common in lining BOF furnaces.

After reaching the temperature of 1680°C and 1700°C, the charge is liquid and the melting stage completed; the melt was then poured into an experimental slag pot and then transferred by a crane to a turntable and tilting platform. Through an additional rail with digital analytical balance weighing control, it was possible to add several types of additives and granular stabilizers based on SiO₂ and Al₂O₃ to adjust the chemical composition, thus modifying its basicity and alumina content.

After this “slag pot metallurgy” step, the samples were tapped manually through a metallic shell into specific molds/devices, with different cooling rates. Figure 1 shows experimental process flow to obtain molten BOF slag modified, with the respective orders of magnitude of the temperatures involved in each step.

2.3 Experimental Devices for Slag Cooling and Evaluated Cooling Rates

Modified slags produced in the metallurgical reactor through the addition of modifying agents had samples cooled in different ways in order to investigate their effect on the crystallization of the modified slag. Three experimental cooling devices were used as follows:

2.3.1 Device 1 - refractory sleeve, thermally insulated at base - slow cooling (1° C/s)

It is a cylindrical ceramic sleeve cast at both ends, supported on a refractory base, as shown in Figure 2, having been prepared on the laboratory bench. This device is characterized by slow cooling, and through measurements

by thermocouples, a cooling rate of less than 1 °C/s was evaluated during the experiments.

2.3.2 Device 2 - refractory sleeve, cooled in a copper base - medium cooling (5°C/s)

The slag is poured into a system comprising a ceramic mold, which receives liquid slag disposed on a water-cooled chute. The same cylindrical ceramic sleeve in device 1 is used, but now rests on a copper base cooled internally by water.

Thermocouples were inserted into the mold, in order to record the cooling rates of the modified slag from high cooling rates (near the shell) to lower rates (region away from the shell). Figure 3 shows a schematic in the glove placed on the mold and filled with slag.

2.3.3 Device 3 - circular cooled mold - quick cooling (21 °C/s)

Figure 4 shows the circular cooled mold for quick cooling, where it can basically be described as a copper mold, subjected to intense heat exchange by cooling with water, during the collection and pouring step of the liquid slag sample. For the calculation of the cooling rate of liquid slag cast in the circular shell, a computational simulation was performed with COMSOL Multiphysics™ software.

2.4 Chemical Analysis and X-Ray Diffraction Rietveld (XRD-Rietveld)

2.4.1 Chemical analysis

Part of the aliquots obtained from the samples, which, after milling and homogenizing, were prepared for analysis by the X-Ray fluorescence spectrometry method

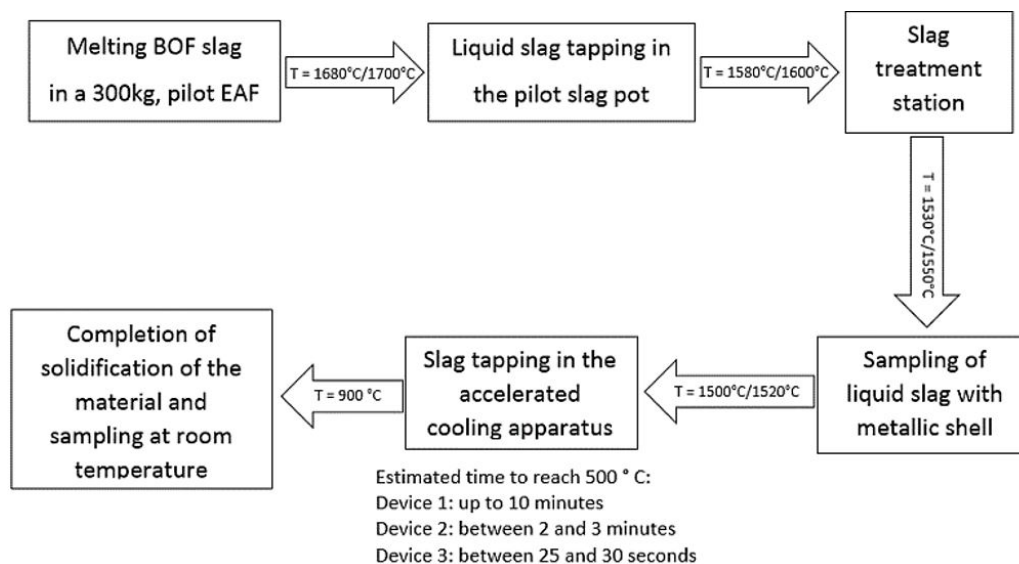


Figure 1. Experimental process flow and temperature evaluation.

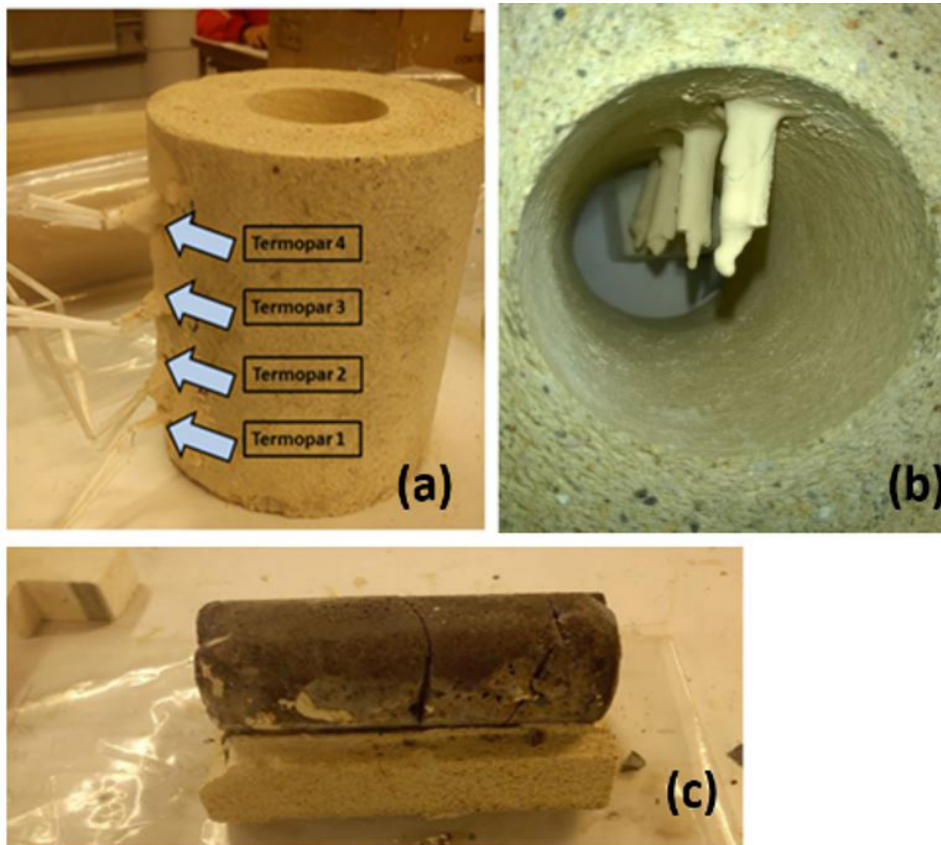


Figure 2. (a) Refractory sleeve, being prepared - Termopar = Thermocouple (b) Thermocouple positioning inside (c) Solidified slag after the experiment.

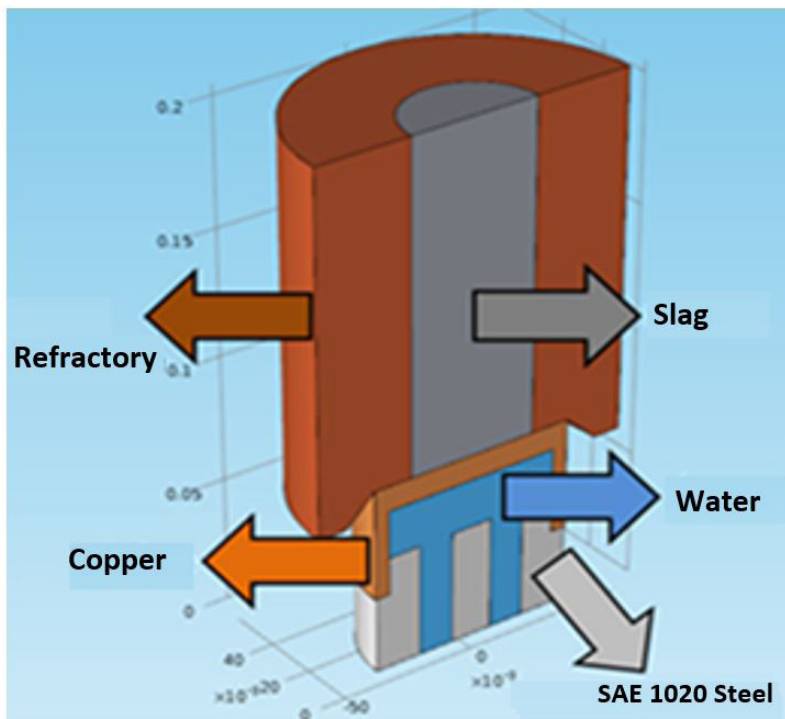


Figure 3. Cooling at a copper base, cooled internally by water - medium cooling (5°C/s).

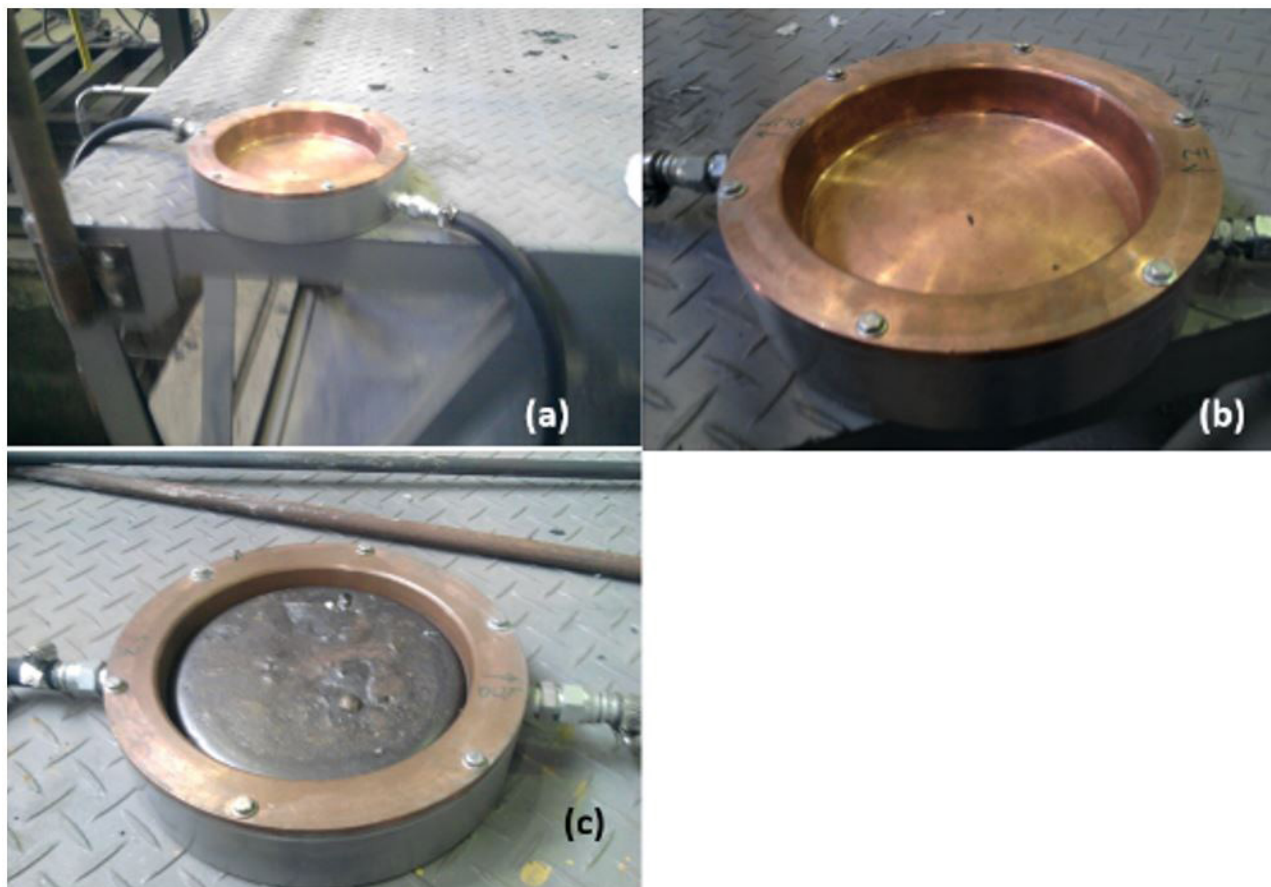


Figure 4. (a) and (b) Construction details of the circular cooled mold, highlighting the inlet and outlet hoses; (c) Modified and totally solidified slag sample.

using PANalytical™ MiniPal equipment. The Fe^{3+} content was calculated by the difference between the total iron, Fe^{2+} and metallic iron.

2.4.2 X-ray diffraction Rietveld (XRD-Rietveld)

The remaining part of the aliquots described in 2.4.1 *Chemical Analysis*, in the form of powders, were analyzed by X-Ray diffraction (XRD) in Rigaku™ WindMAX 1000 diffractometer, using $Cu\ K\alpha$, 40 kV, 20 mA and scanning of $0.2^\circ/\text{min}$.

2.5 FactSage® Thermodynamic Calculation

Thermodynamic calculations were performed in software FactSage® 7.0 to predict the phases that form during the solidification of the slag. In these calculations, the tool used was the *Equilib* with *FToxid* and *FactPS* data bases. *FToxid-SlagA* database was used for the calculation of liquid solutions. For solid solutions *FToxid-MeO_A* presented as RO phase in the results; *FToxid-bC₂S*, *FToxid-aC₂S* and *FT-oxid-Mel* presented as Melilite; and *FToxid-OlivA* presented as Olivine.

The calculations were based on the chemical compositions presented in Table 2. The gas phase was not considered in the calculations. The results obtained by the thermodynamic simulation were compared with the results of the XRD analysis.

3 RESULTS

3.1 Chemical Composition

The chemical compositions for the fifteen tests slag modification are presented in Table 2, parameterizing the quantities of CaO, SiO_2 , FeO, MgO, MnO, Fe_2O_3 and Al_2O_3 values in 100%, which are used for thermodynamic simulation as previously stated. The values of basicity for the Crystalline group trials are in the range of 0.7 to 1.3 and the Al_2O_3 content in the range of 2.2 to 4.7%; for the Amorphous group trials, basicity was obtained in the range of 0.9 to 1.2 and Al_2O_3 levels in the range of 10.0 to 12.5%. Table 3 shows the cooling conditions of the slag for each heat performed.

3.2 Thermodynamic Calculation and XRD-Rietveld analysis

In Figure 5, the thermodynamic simulation of Heat #1 (Crystalline trials) is presented, showing the phases present between liquidus and solidus temperature, assuming thermodynamic equilibrium, in a theoretical process of infinite time solidification. This pattern of thermodynamic solidification has been followed in all heats tested in this

work. It is shown in Figure 6, where the XRD-Rietveld of Heat #1 (Crystalline trials) the phases present, where no amorphous is detected. Same in Figure 7, for Heat #13, (Amorphous trials), where a 25,1% amorphous was detected.

Using this same comparison procedure for the other heats tested, with all data compiled, the results for Merwinite, Melilite, Monticellite and Wüstite are shown in Figures 8, 9, 10, and 11, for comparative visualization.

Table 2. Chemical composition, % (COSIPA, Crystalline, and Amorphous group trials)

		CaO	SiO ₂	FeO	MgO	MnO	Fe ₂ O ₃	Al ₂ O ₃	C/S
COSIPA'S BOF slag		40.3	10.5	19.3	9.1	4.7	14.4	1.8	3.9
Crystalline group trials	Heat #1	35.5	32.6	11.7	9.1	4.3	3.7	3.1	1.1
	Heat #2	25.0	36.1	18.5	5.8	3.0	8.0	3.6	0.7
	Heat #3	30.6	27.0	19.9	8.0	3.7	6.2	4.7	1.1
	Heat #4	32.6	30.1	17.5	8.5	3.9	4.5	3.0	1.1
	Heat #5	34.1	31.2	14.9	8.2	4.0	3.6	4.1	1.1
	Heat #6	34.3	31.7	14.4	8.4	4.0	3.6	3.6	1.1
	Heat #7	33.2	32.2	16.2	7.5	3.6	4.9	2.4	1.0
	Heat #8	29.4	32.3	20.1	7.1	3.5	5.4	2.2	0.9
	Heat #9	32.2	29.8	19.3	8.0	3.8	3.6	3.2	1.1
	Heat #10	32.9	29.1	18.9	8.3	3.8	4.3	2.8	1.1
	Heat #11	37.8	29.6	13.3	8.7	4.5	2.7	3.5	1.3
	Heat #12	38.4	28.9	12.6	10.0	4.4	3.0	2.8	1.3
Amorphous group trials	Heat #13	39.0	32.6	2.5	9.9	3.4	0.3	12.5	1.2
	Heat #14	35.0	32.1	7.2	9.7	4.1	1.9	10.0	1.1
	Heat #15	32.3	34.7	6.7	8.0	3.6	2.8	12.1	0.9

Table 3. Slag cooling conditions for each test

Cooling Apparatus	Trials
Device 1 – 1°C/s	Heat #3
Device 2 – 5°C/s	Heats #1, #2, #5, #7 and #10
Device 3 – 21°C/s	Heats #4, #6, #8, #9, #11, #12, #13, #14 and #15

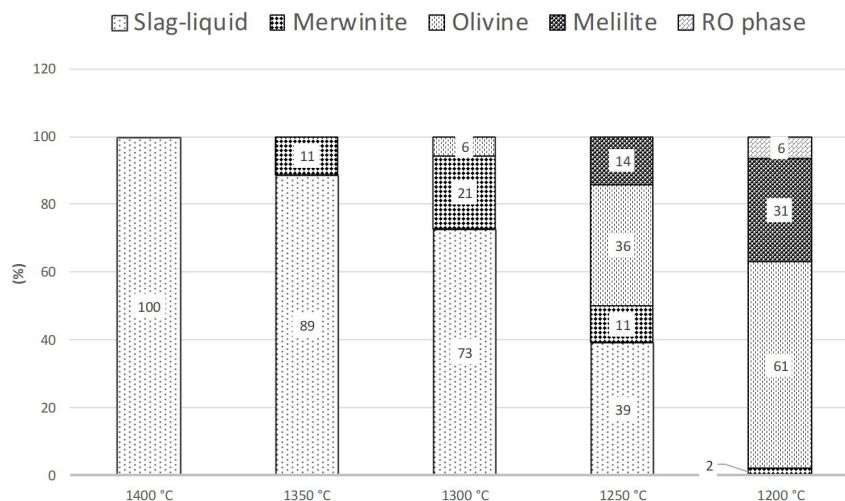


Figure 5. Heat #1-Thermodynamic Simulation. T_{Liquidus} (°C) = 1400; T_{Solidus} (°C) = 1200. Crystalline trials.

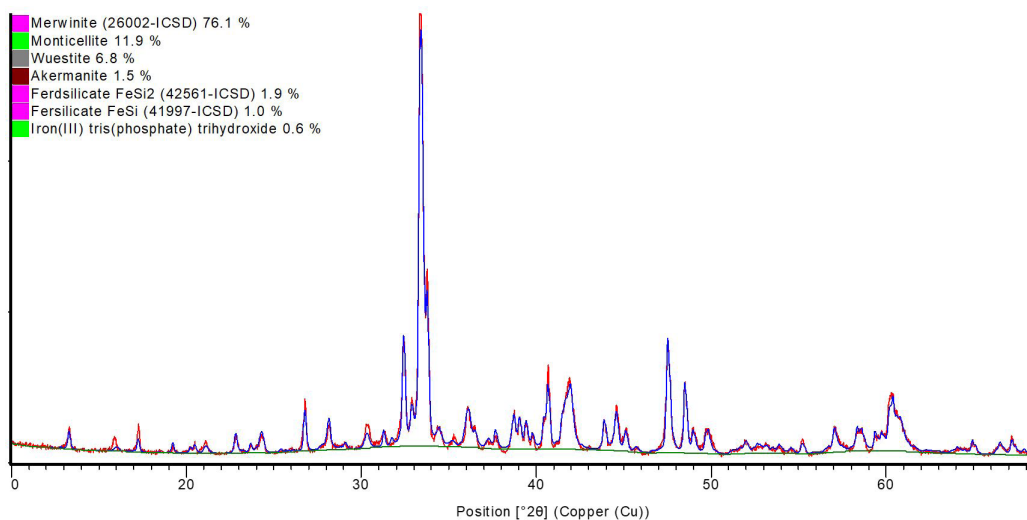


Figure 6. Heat #1 - XRD-Rietveld analysis. T_{Liquidus} (°C) = 1400; T_{Solidus} (°C) = 1200. Crystalline trials.

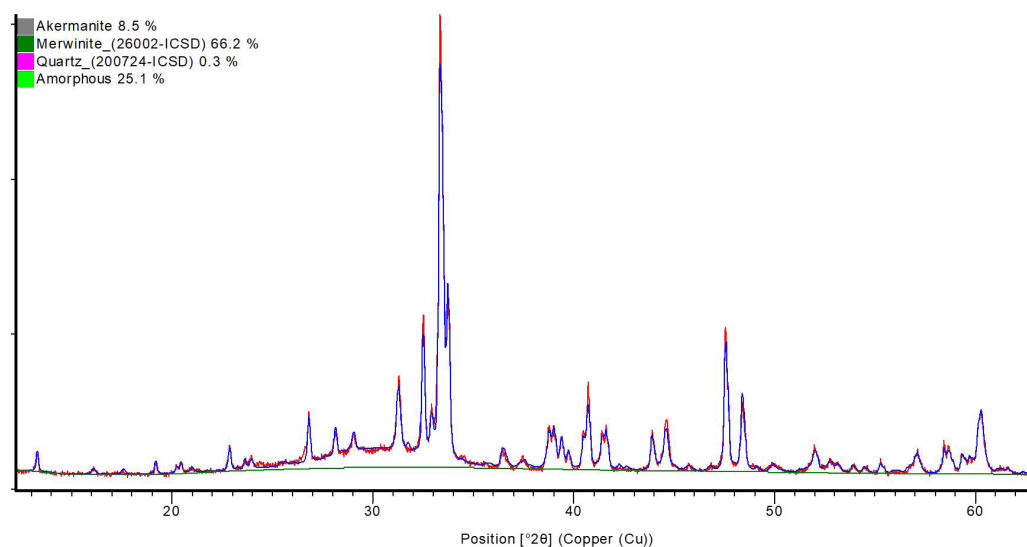


Figure 7. Heat #13 - XRD-Rietveld analysis. T_{Liquidus} (°C) = 1400; T_{Solidus} (°C) = 1200. Amorphous trials.

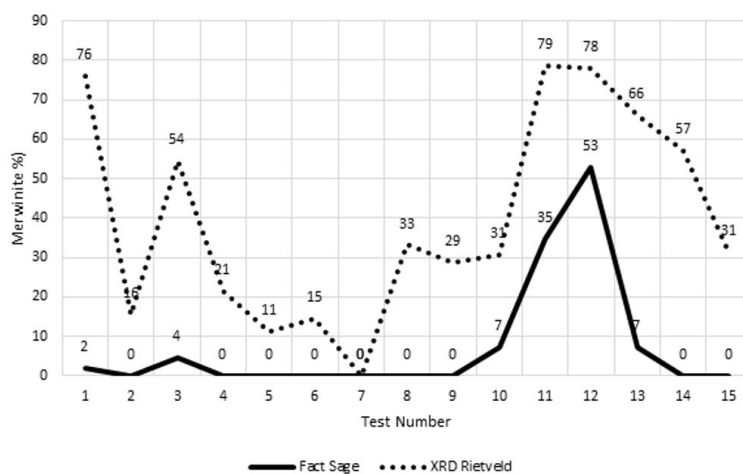


Figure 8. XRD-Rietveld results compared with FactSage® Thermodynamic Simulation for Merwinite.

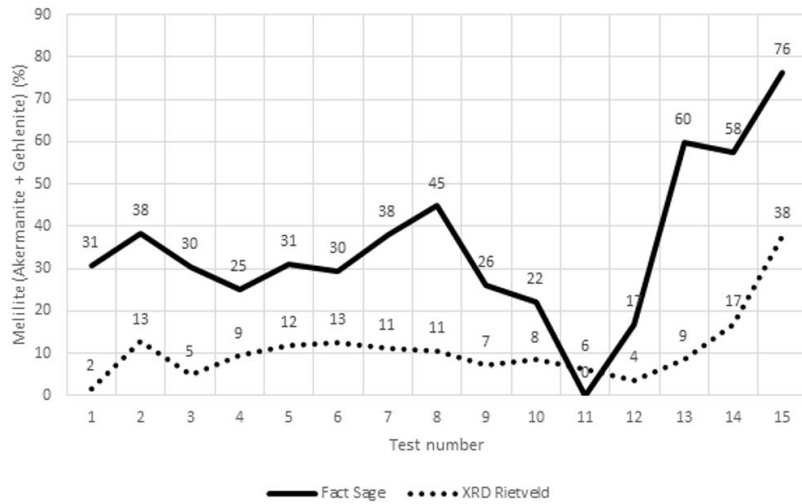


Figure 9. XRD-Rietveld results of compared with FactSage® Thermodynamic Simulation for Melilite (Akermanite + Gehlenite).

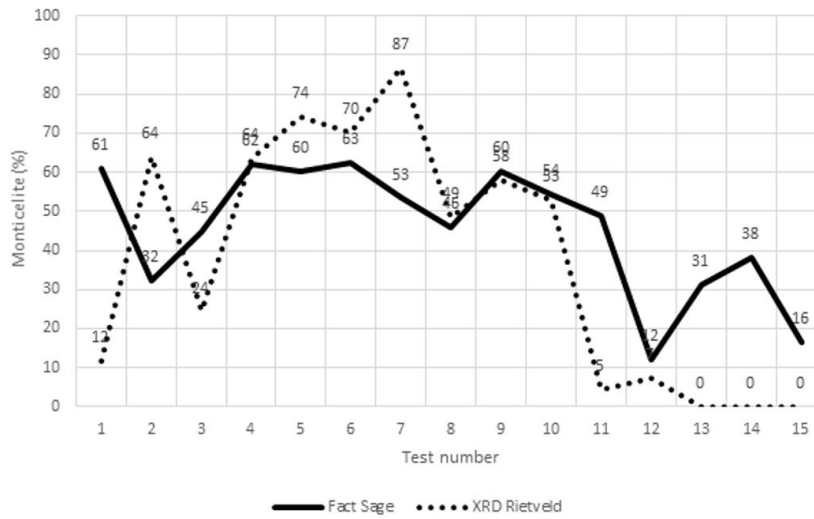


Figure 10. XRD-Rietveld results of compared with FactSage® Thermodynamic Simulation for Monticellite.

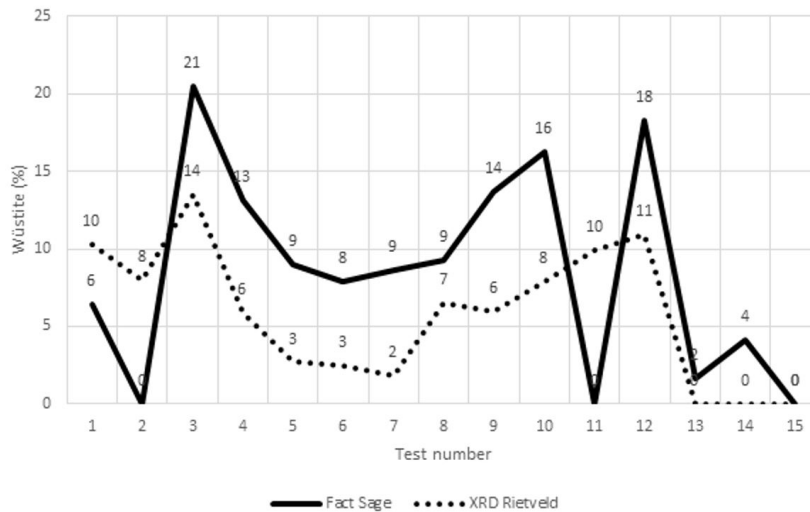


Figure 11. XRD-Rietveld results of compared with FactSage® Thermodynamic Simulation for Wüstite.

Heats from Crystalline group trials did not present amorphous phase. Meanwhile, heats # 13, 14 and 15 (Amorphous trials), presented 25%, 26% and 31% amorphous phase respectively.

4 DISCUSSION

4.1 Theoretical Thermodynamic Slag Solidification

During the solidification process by thermodynamic simulation, represented schematically by Figure 5, Heat # 1 (crystalline trials), Olivine solid solution has a predominance below 1300°C; Monticellite and Kirschsteinite are the predominant solution phases in this Olivine solution. Ca_2SiO_4 and Glaucocroite are also present at lower temperatures, and at 1200°C, these phases are distributed around 40% for Monticellite, 28% for Kirschsteinite, 15% for Larnite and Glaucocroite in Olivine solid solution.

The solid solution of Melilite begins to form below 1250°C, and contains predominantly Akermanite and Gehlenite in solution, and at 1200°C an average proportion of 37% is estimated for Akermanite and 21% for Gehlenite; at this temperature, we reported the possibility of precipitation of Iron-Akermanite ($\text{Ca}_2\text{FeSi}_2\text{O}_7$) in the proportion of 22%. At the temperature of 1200°C the solid oxide solution, RO phase becomes stable with predominance of FeO (53%) and Fe_2O_3 (32%).

4.2 XRD-Rietveld in Comparison with FactSage® Thermodynamic Simulation

It was considered as a criterion of comparison between the methods, that the majority phase within a solution by thermodynamic simulation would be the constituent comparable to the phase detected by XRD-Rietveld.

In Figures 8, 9, 10, and 11 the results obtained from the precipitated phases are compared by FactSage® thermodynamic simulation in T_{solidus} and XRD-Rietveld diffractograms. The typical crystalline phases found in the thermodynamic simulation for this series of experiments are confirmed by XRD-Rietveld. These phases are: solid precipitate from Merwinite, Olivine solid solution containing Monticellite, solid solution of Melilite containing Akermanite and Gehlenite, solid RO phase solution containing Wüstite.

Andradite and Anortite solids precipitates were not detected XRD-Rietveld, and a small amount of Akermanite was detected in comparison with the thermodynamic simulation, and as a result, the simulation did not predict Gehlenite, unlike XRD-Rietveld, which did not detect Wolastonite. Anortite, 5% and 7% (in Heats 2 and 15) and Andradite, 22% (Heat # 2) and Wollastonite solid precipitates, 3% (in Heat # 2), CaFe_2O_4 Spinel, were predicted by thermodynamic simulation, but these precipitates were not detected in XRD-Rietveld.

The comparison of the phase prediction by the thermodynamic equilibrium model and XRD-Rietveld was shown to be partially consistently coherent, with reproducibility of the thermodynamic theoretical results, reinforced with the physical verification of the XRD-Rietveld. Quantitatively, however, the comparative results between the phases showed erratic dispersions between the percentage obtained by simulation and XRD-Rietveld. This can be explained by the fact that the solidification in the devices is not done under equilibrium conditions (as opposed to the thermodynamic simulation) and also because of the heterogeneities caused by the variations in the cooling velocity that occurs between the (cooler) wall and the nucleus (warmer) forming crystals of different phases and sizes.

4.3 Evaluation of Crystalline and Amorphous Fraction

4.3.1 Crystalline trials

All heats in this group had only crystalline phase, independent of the cooling rate applied. In this group, the basicity was between 0.7 and 1.3 and the maximum content of Al_2O_3 was 4.7%, where the XRD-Rietveld do not indicate the presence of amorphous phase.

4.3.2 Amorphous trials

In this case, all the heats of this group presented both crystalline phase and amorphous phase, for contents above 10% Al_2O_3 . In this group, the basicity was between 0.9 and 1.2, similar to the crystalline trials and the Al_2O_3 content was between 10 and 12.5%, where the diffractograms indicated the presence of amorphous phase in heats # 13, # 14 and # 15. The influence of the cooling rate of 21 °C/s on amorphous phase formation is not conclusive.

CONCLUSIONS

The main conclusions can be summarized as follows:

1. Solidification of BOF modified slag resulted in several predominant crystalline phases: Olivine solid solution, Melilite and RO phase, and solid precipitate of Merwinite.
2. The phases found in the XRD-Rietveld analyzes confirm the thermodynamic simulation for this series of experiments in a qualitative way; but in a quantitative way, the results showed erratic dispersions, with a lower percentage bias for the XRD analyzes.
3. Heats tested with basicity below 1.1 and Al_2O_3 content below 5%, favor the formation of crystalline phases and absence of amorphous phase. With cooling rates up to 21 °C/s, for this group (Crystalline trials), there is no evidence of amorphous phase formation.

4. Heats tested with basicity below 1.2 and Al_2O_3 content between 10.0% and 12.5% favors the formation of both crystalline (majority) and amorphous phases (between 25% and 31%), .
5. With cooling rates of 21 °C/s for this group of heats (Amorphous trials), we cannot conclude the influence of this variable in the formation of amorphous phase.
6. There was no free CaO phase formation or free MgO, thus reducing the possibility of the expansion effect after hydration. There were also no phase formation with cementitious properties such as Alite and Belite in this process of pyrometallurgical modification of BOF slag.

References

- 1 Reddy AS, Pradhan RK, Chandra S. Utilization of Basic oxygen Furnace (BOF) slag in the production of a hydraulic cement binder. *International Journal of Mineral Processing*. 2006;79(2):98-105. <http://dx.doi.org/10.1016/j.minpro.2006.01.001>.
- 2 Tsakiridis PE, Papadimitriou GD, Tsvilis S, Koroneos C. Utilization of steel slag for Portland cement clinker production. *Journal of Hazardous Materials*. 2008;152(2):805-811. <http://dx.doi.org/10.1016/j.jhazmat.2007.07.093>.
- 3 Das B, Prakash S, Reddy PSR, Misra VN. An overview of utilization of slag and sludge from steel industries. *Resources, Conservation and Recycling*. 2007;50(1):40-57. <http://dx.doi.org/10.1016/j.resconrec.2006.05.008>.
- 4 Soykan HŞ. Cementitious material production from hot mixing of ironmaking and steelmaking slags. *Mineral Processing and Extractive Metallurgy*. 2006;115(4):229-233. <http://dx.doi.org/10.1179/174328506X128850>.
- 5 Engström F, Pontikes Y, Geysen D, Tom Jones P, Björkman B, Blanpain B. Review: hot stage engineering to improve slag valorization options. In: 2nd International Slag Valorization Symposium; 2011 April 18-20; Leuven, Belgium. Leuven: Katholieke Universiteit Leuven; 2011. p. 231-251.
- 6 Ferreira JB No, Fredericci C, Faria JOG, Chotoli FF, Ribeiro TR, Malynowskyj A, et al. Modification of basic oxygen furnace slag for cement manufacturing. *Journal of Sustainable Metallurgy*. 2017;3(4):720-728. <http://dx.doi.org/10.1007/s40831-017-0133-5>.
- 7 Yao-Hung T, Yu-Chen L, Bor-Liang S. Application and Breakthrough of BOF Slag Modification. *China Steel Technical Report*. 2015;28:46-51.
- 8 Ferreira JB No, Faria JOG, Fredericci C, Chotoli FF, Silva ANL, Ferraro BB, et al. Modification of molten steelmaking slag for cement application. *Journal of Sustainable Metallurgy*. 2016;2(1):13-27. <http://dx.doi.org/10.1007/s40831-015-0031-7>.

Received: 5 Nov. 2017

Accepted: 11 Jun. 2018